Journal of Physics:
Conference Series

PURPOSE-LED PUBLISHING™

PAPER • **OPEN ACCESS**

Turbulence Impact on Wind Turbines: Experimental Investigations on a Wind Turbine Model

To cite this article: A Al-Abadi *et al* 2016 *J. Phys.: Conf. Ser.* **753** 032046

View the article online for updates and enhancements.

You may also like

- Structure of Offshore Low-Level Jet Turbulence and Implications to Mesoscale-to-Microscale Coupling
Balaji Jayaraman, Eliot Quon, Jing Li et al.
- Comparison of the Behavior of the FM01-LC Reactor with and without Turbulence Promoter Using CFD
Locksley Fabian Castañeda Ulloa, Rene antaño Lopez and José Luis Nava
- The turbulence scales of a wind turbine wake: A revisit of extended k-epsilon models
M P van der Laan and S J Andersen



This content was downloaded from IP address 178.237.49.176 on 16/12/2025 at 13:06

Turbulence Impact on Wind Turbines: Experimental Investigations on a Wind Turbine Model

A Al-Abadi[1,2,4], Y J Kim[2,3] Ö Ertunç[5] and A Delgado[2,3]

[1] SGB Power Transformers, R & D Dept., Regensburg, Germany
[2] Institute of Fluid Mechanics, FAU Erlangen-Nuremberg, Germany
[3] Institute of Fluid Mechanics, FAU Busan, South Korea
[4] AlKhwarizmi College of Engineering, University of Baghdad, Iraq
[5] Ozyegin University, Mechanical Engineering Dept., Istanbul, Turkey

Abstract. Experimental investigations have been conducted by exposing an efficient wind turbine model to different turbulence levels in a wind tunnel. Nearly isotropic turbulence is generated by using two static squared grids: fine and coarse one. In addition, the distance between the wind-turbine and the grid is adjusted. Hence, as the turbulence decays in the flow direction, the wind-turbine is exposed to turbulence with various energy and length scale content. The developments of turbulence scales in the flow direction at various Reynolds numbers and the grid mesh size are measured. Those measurements are conducted with hot-wire anemometry in the absence of the wind-turbine. Detailed measurements and analysis of the upstream and downstream velocities, turbulence intensity and spectrum distributions are done. Performance measurements are conducted with and without turbulence grids and the results are compared. Performance measurements are conducted with an experimental setup that allow measuring of torque, rotational speed from the electrical parameters. The study shows the higher the turbulence level, the higher the power coefficient. This is due to many reasons. First, is the interaction of turbulence scales with the blade surface boundary layer, which in turn delay the stall. Thus, suppressing the boundary layer and preventing it from separation and hence enhancing the aerodynamics characteristics of the blade. In addition, higher turbulence helps in damping the tip vortices. Thus, reduces the tip losses. Adding winglets to the blade tip will reduce the tip vortex. Further investigations of the near and far wake-surrounding intersection are performed to understand the energy exchange and the free stream entrainment that help in retrieving the velocity.

1. Introduction

In general, wind turbines are designed by assuming a uniform laminar incoming flow. However, wind turbines may operate under the influence of the turbulent atmospheric boundary layer. Thus, wind turbines are exposed to different levels of turbulence depending on the time dependent weather conditions and the site such as: terrains and location in a wind-farm. Therefore, understanding the impact of the turbulence level on the performance of the wind turbine as well as the downstream wake are crucial for the efficient design and operation of Horizontal Axis Wind Turbines (HAWTs).

The incoming wind to HAWTs changes its speed and direction stochastically with time. Wind turbines that are exposed to high turbulence levels are prone to extreme fluctuating of both attack and yaw angles. Further, time scales of wind fluctuations and sudden changes of wind properties can be very short and very high in amplitude. Thus, grasping the response and improving the reaction to those


Content from this work may be used under the terms of the Creative Commons Attribution 3.0 licence. Any further distribution of this work must maintain attribution to the author(s) and the title of the work, journal citation and DOI.
Published under licence by IOP Publishing Ltd

changes by different means are decisive for modern wind turbines not only to exploit as much power as possible but also to stabilize energy production and prevent any damage of the turbine.

The effect of atmospheric turbulence has been investigated in many studies. Barthelmie[1] proved that for a large offshore wind farm the losses in the power due to turbine wakes can reach up to 20%. In contrary, Hansen[2] showed that at a specified wind farm the ambient turbulent intensity has a linear influence on increasing the total wind farm efficiency, for the wind speed range 7-8 m/s. Further study in a wind farm was conducted by Türk[3], which proved both power output and loads on turbine blades are increasing with the increment of turbulence intensity levels.

Many studies have shown that turbulence serves in delaying the flow stall on the suction surface of the blade. Swalwell et al.[4], studied the influence of turbulence intensity on the aerodynamics performance of the thick airfoil NACA0021, which is normally placed at the root of wind turbine blades that is the first stalled part of the blade, by subjecting it to different levels of turbulence intensities. As a result, the increasing turbulence was found to delay stall until higher angle of attack in a way that is consistent with the delayed stall seen on HAWT. This was confirmed by Delnero[5] for different airfoils and by Watkins[6] for low Reynolds number wings due to the impact of the turbulence intensity on the laminar separation bubbles. Kamada[7], proved experimentally that the turbulence flow prevents the flow separation on the airfoil surface and hence delays the stall. Whereas in another experimental work conducted by Maeda[8], it is found that the main flow turbulence has a direct impact on the wind turbine wake due to entrainment, which helps to recover the velocity deficit. Therefore, higher turbulence intensity leads to higher power output of the downstream wind turbine.

In addition to the incoming wind turbulence, the effect of the upstream turbine on the wake velocity and added turbulence intensity is still obvious even at a distance of fifteen times the rotor diameter, as presented by Chamorro[9]. The added wake turbulence has been estimated in many semi-empirical models. Frandsen[10] proposed a model for estimating the added turbulence by taking into account the wind-farm layout and additional surface roughness generated by the turbines. Whereas, Wessel[11] developed a semi-empirical model for calculating turbulence intensity inside offshore wind farms, which is taken from the wind speed deficit profile. It takes into account the wake superposition, interference and meandering to calculate the incidence of the turbulence intensity on each rotor within the farm for various wind direction and speed.

Additional challenges associated with turbulence such as unsteady aerodynamics forces, are investigated by Luhur[12]. His study aimed to model the dynamic lift and drag stochastically under turbulent conditions. Changes in the angle of attack at time scales of one second and less was investigated,[13]. The main focus laid on high frequent fluctuations in the wind and the resulting changes in the angle of attack. Other challenges, like the influence of the short-scale turbulence was considered by Peinke[14]. He showed that a small-scale atmospheric turbulence, which can results from wind gusts, can statistically arise the anomalous probabilities.

In the present study we try to highlight the turbulence impact on the performance and wake of the HAWT. This is done by exposing an efficient wind turbine model to different turbulence levels generated by two static grids in a wind tunnel. The study has shown that turbulence can improve the turbine performance by different possible means. This is obtained after a precise measurement for the reference upstream velocity. In addition, we could perform an intensive investigation of the tip vortex.

2. Experimental Setup

In order to highlight the impact of the turbulence on the performance of the HAWT, an optimized laboratory scale wind turbine is produced by using the TMASO method. TMASO is an optimization method that changes the blade shape in order to capture the maximum power from the wind under the torque-rotational speed constraint of the drive unit. The method is called as Torque Matched Aerodynamic Shape Optimization (TMASO)[15].

It is important to have a turbine with high efficiency to study the influence of turbulence, so that, it

is possible to understand the influence of turbulence. The blade sections are constructed of SG6043 profile since it provides a high-lift at low-Reynolds numbers.

Tests are conducted in the closed loop wind tunnel of the Institute of Fluid Mechanics (LSTM) at the Friedrich-Alexander-University by exposing the wind turbine to turbulence with various levels and length scales contents.

The model is connected to a generator. An electrical circuit provides a precise control of consumed power by the load (R_{load}), which is equal to the generated total electrical power P_t by the generator is used. It is designed in such a way that the power consumption of the load can be adjusted by adjusting the current (I) passing through it. The R_{load} can also be replaced to extend the measurement range or to have the desired operation range.

In order to find the mechanical power extracted by the rotors from the wind, it is necessary to know the relation between the measured electrical quantities, torque T_{drive} and rotational speed n of the driving unit (generator). These relations are found by using another set-up. In which, the generator is connected to a servo motor that keeps the rotational speed constant. The power measurement circuitry is the same as the one used in wind-tunnel tests. An arm is connected at one end to the generator and at the other end placed onto a balance, so that torque at the set conditions can be measured.

The measurements delivers the $T_{drive} - n$ relation at a constant R_{load} and I. For chosen values of R_{load}, I and of wind velocity, the generator rotates with a certain rotating speed and produces a potential difference E, which are in turn used to calculate the shaft power P_s. Hence, the measurements of E at constant R_{load} and I in the wind-tunnel tests are used to calculate $T(E, I, R_{load}), \omega(E)$ and the shaft power P_s :

$$P_s = T(E, I, R_{load})\ \omega(E)$$

where,

$$\omega = \frac{2\pi n}{60}$$

The power of the wind passing through the turbine blades is:

$$P_s = \frac{1}{2}\rho v_1^3 A$$

Thus, the aerodynamic power coefficient C_p can be calculated as:

$$C_p = \frac{P_s}{P_w}$$

In the experiments C_p values are found out as a function of the tip speed ratio λ by varying the wind-speed. Details of the wind turbine setup that consists of rotor, generator, mechanical tower, nacelle and electrical circuitry are explained in[16]. The turbulence is generated by using two static grids having mesh sizes 8mm (fine) and 40mm (coarse),cf. Figure 1.

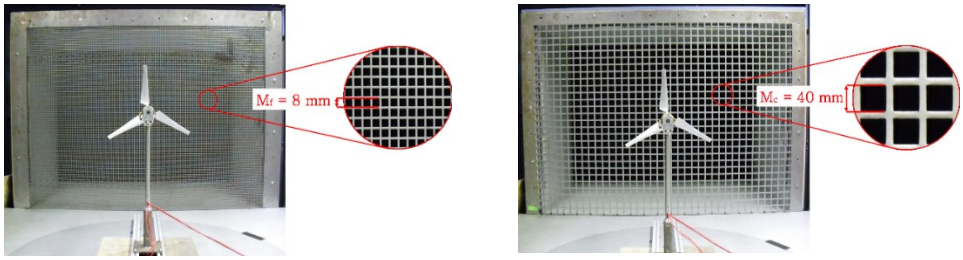


Figure 1. Optimized wind-turbine exposed to two grids (fine and coarse) in the wind tunnel

Hence, two mainly different turbulence scales are obtained at the inlet of the wind tunnel. In addition, the distance between the wind-turbine and the grid is adjusted to have 9 different positions, thus 9 sub-turbulence intensities for each grid, cf. Figure 2.

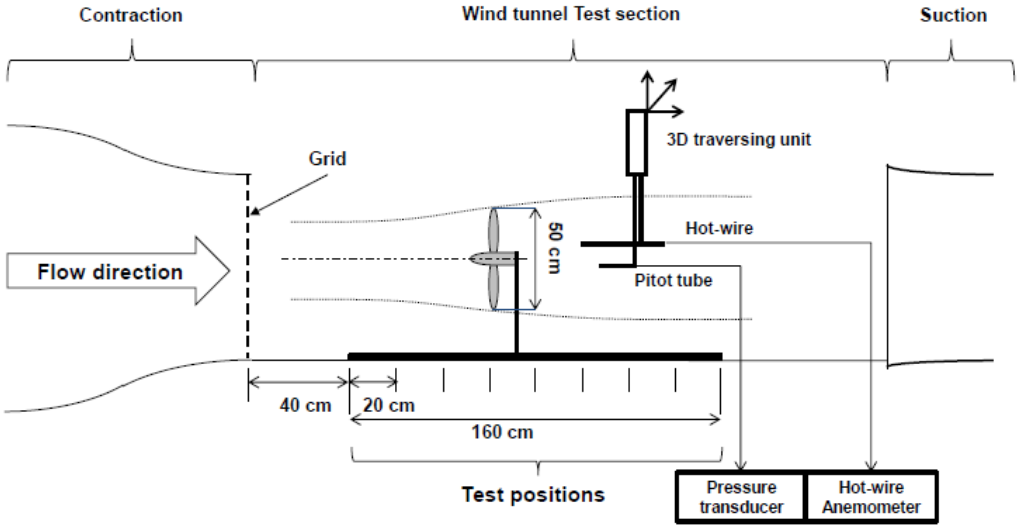


Figure 2. Schematic of the experimental rig in the wind

The Pitot-static tube is fixed on the 3-D traversing system alone for the velocity measurements and beside the hotwire probe for the calibration of the hot- wire.

The velocity measurement, for up and downwind velocity distribution investigation, is performed by measuring the difference in static and total pressure with a SETRA differential-pressure transducer connected to the Pitot-static tube and by applying the Bernoulli equation.

To conduct turbulence measurements, a single normal hot-wire connected to an anemometer unit with a constant-temperature bridge CTA is employed. The wire has a length of 1mm and a diameter of 5μm. Velocity calibration of the employed hot-wire is performed at the test section near the inlet of the wind tunnel test section. During the calibration and the measurements, the temperature of the flow is measured with a PT100 temperature sensor in order to correct the measured data for temperature drifts. The hot-wire signals, pressure transducer signal and temperature signal are acquired by a 16-bit A/D converter (NI 6059E DAQ card) installed in a personal computer. The data is recorded for further analyses of spectra and autocorrelation.

The sampling rate (SR) for the measurements is chosen in such a way that wide scales of fluctuations can be acquired. SR is set to be 20 kHz, with a measuring time period of t=120s. Thus, the acquired 2.4 million data can provide lower uncertainty turbulence scales and of the turbulence intensity (TI) measurement. Turbulence field generated by the two grids are characterized in the absence of wind turbines. Hot-wire measurements are also used to monitor the turbulent wake of the wind turbines.

The reference wind speed is set to free-stream velocity of $v_1 = 12m/s$, which is the design speed for the turbine model. It leads the designed wind turbine type to belong to Wind turbine class S and SWT class S according to IEC standard[20, 21]. Measurements of velocity are taken in an area around the tips of the normalized axial distances of x/D = 0.2, 0.4 and 0.6. For each x/D, the radial direction with the highest fluctuation in velocity is chosen and directly compared to the corresponding y/D for different turbulence levels.

3. Experimental Investigations

3.1. Grid Generated Turbulence

To quantify the turbulence created by the grids, hot-wire measurements are taken inside the test section.

The turbulence level increases with the installation of the fine grid at the entrance of the test section.

Turbulence intensity, stays constant over the whole test section at $TI = 0.007$ when it is measured without the grid. The same effect, but in a higher level of turbulent intensity, is depicted when using of the coarse grid. The range of the turbulence intensity is from 0.114 to 0.032 for x values of 40 and 180 cm respectively. The turbulence decays in the flow direction, Figure 3. The turbulence is shown to be nearly isotropic in prior investigations for the same wind tunnel and the same grids[17].

Since the grid turbulence is nearly isotropic, the measurements are restricted to the longitudinal direction. Hot-wire and Pitot-tube are placed in the center of the flow and traversed in the flow direction during the measurements. It is known that mean velocity distribution has strong inhomogeneity in the proximity of the grid [17]. For this reason, measurements are conducted only for $x \geq 40$. Steps of $\Delta x = 20cm$ are chosen as a compromise between accuracy and expenditure.

The energy spectrum at hot-wire distance from the grid of $x=120cm$ at the design free-stream wind velocity is depicted in Figure 4. The position of $x=120cm$ is selected since it satisfies both the isotopy of the free-stream turbulence and the sufficient down-stream distance for wake and hence tip-vortices development.

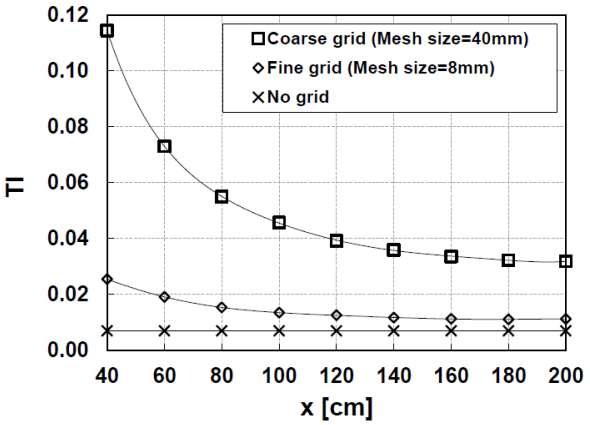


Figure 3. Intensity of grid-generated turbulence along the test section for the three grid cases at average wind velocity $v_1 = 8 - 16m/s$

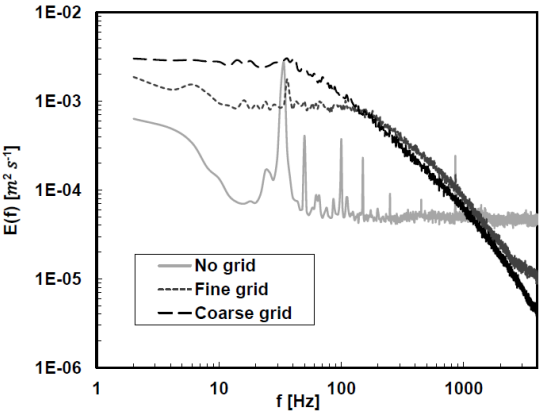


Figure 4. Spectra E(f) distribution with eddies frequencies (f) at different grids with the design free-stream wind velocity $v_1 = 12m/s$, hot-wire position of x=120cm, with the absence of wind turbine.

3.2. Power Coefficient

The optimized turbine model is exposed to fine and coarse grids and varying wind speeds in a range from 10.5 to 13.5 *m/s*. This will guarantee testing the design and the off-design conditions, since the turbine is designed for wind velocities of 12 *m/s.*

To study the influence of a wide range of turbulence intensities, the turbine is mounted on an axial traverse to allow moving it from x = 60 *cm* to x = 120 *cm* distance from the inlet of the test section in steps of $\Delta x = 20\ cm$, Figure 2.

Figure 5 shows the power coefficient C_p as a function of λ along the flow direction for the wind turbine at different positions. This is performed by moving the turbine towards the grid to face higher *TI*'s. The free flow turbulence (no grid) is added to the figure for comparison. The power coefficient increases as the turbulence level increases. The tip speed ratio increases too, this indicates that the rotational speed increases since the reference oncoming wind velocities are same.

The high turbulent intensity case (coarse grid) is shown in Figure 6. In comparison to the medium turbulence levels, high turbulence shows a higher performance. Thus, performance curves are shifted to the right for both turbines due to higher rotational speeds. The performance curves in coarse grid are

closer to each other than those in the fine grid. In the coarse grid there is a large increment of C_p at the turbine position of $x = 120cm$, which corresponds to the minimum turbulence position, as compared to the C_p at the same position of the fine grid. Performance with coarse grid reaches 52%, which means there is less room for further improvement towards Betz limit when compared to to the maximum of 48% of fine grid results. Nevertheless, the values of C_p of the coarse grid for all distances are more than the fine grid at the same turbine positions.

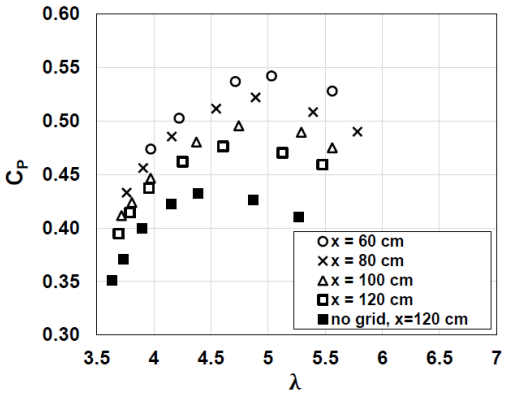


Figure 5. The trend of C_p values at varying turbine axial positions with fine grid

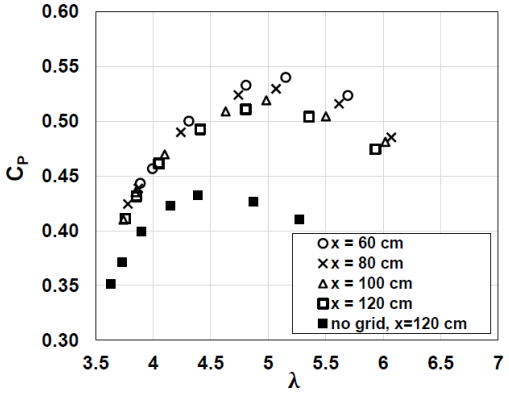


Figure 6. The trend of C_p values at varying turbine axial positions with coarse grid

3.3. Velocity distribution

The velocity distribution around the turbine is measured during the operation of the turbine to provide insight of the upwind and downwind velocities deficits and the wake development. The wind turbine is set on a wind tunnel test section at a sufficient distance, which is chosen to obtain the reference incoming wind speed. The first indication for the accurate reference wind velocity is when its distribution across the far upwind lateral sections (or section of symmetry) is constant, which implies there is no wind turbine blockage effect. Second indication is when the velocity in axial direction towards the turbine stays constant for a sufficient distance before it then drops, this implies that the axial position of the turbine in relation to the wind tunnel is sufficient to appoint the wind tunnel velocity as a reference. Both requirements are fulfilled at a turbine distance of $x = 120cm$ from the inlet of the test section. All the following measurements are taken at $\mathrm{v}_1 = 12m/s$, which is the design velocity of the turbine.

In Figure 7 it is shown that at a dimensionless ratios of the upwind distance to rotor diameter of $x/D = -1.7$, the lateral y/D distribution of velocity is constant. It will keep constant values in both axial and lateral distributions until we reach the dimensionless upwind distance of $x/D = -1.5$. In the same figure, as we move towards the turbine, i.e. increasing x/D velocity distribution drops and the dropping area becomes wider and wider. This drop is associated with the existence of the turbine, where it extracts the incoming wind kinetic energy and converts it to a mechanical one as well as the rotor stagnation, thus the velocity drops to a value which in turn indicates the turbine performance $C_p = 4\mathrm{a}(1-\mathrm{a})^2$, where a is the axial index factor. The dropping is reduced as we move in the lateral direction and it even exceeds the turbine radius at $\mathrm{y/D} = 0.5$. It is clear in the figure the distance where the velocity deficient is still obvious until $\mathrm{y/D} = 1$.

Figure 8 shows the velocity distribution behind the turbine. Moving away from tip $\mathrm{y/D} = 0.5$ in lateral direction, there is a continuous velocity deficit that exceed the rotor diameter.

At the near weak region x/D = 0.2, starting from $\mathrm{y}/D \approx 0.5$, which is exactly the tip of the turbine rotor, an abrupt increment can be seen clearly. Here is the border between the areas of the extracted wind kinetic energy and the surrounding unaffected flow, which represents the surrounding stream tube.

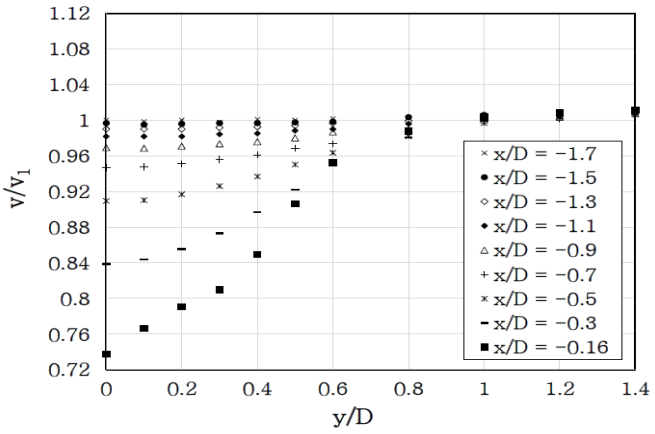


Figure 7. Upwind velocity distribution without grid at $v_1 = 12\ m/s$

It can be seen in the figure an increase in velocity of about 20% compared to the reference (12 m/s, or 1 when normalized to itself). Since the turbine is blocking the flow, the surrounding flow just around the rotor bends around the rotor tips results in a higher flow rate which leads to an increment of the velocity at that region. The region between the edges of the abrupt increase and the points before the increment is the border of the stream tube, in which it the tip vortices have their influence. This region is expanding in the wake and still refer to the wake shear inner and outer boundaries, where the shear resulting from different velocities is appearing. Hence, as we move away from the turbine in axial direction x/D, the influence of the blockage becomes less, and thus, the mixing area becomes wider.

The velocity deficit will extend more outside and the drop becomes more and more flat. It can also be seen that at higher distances from the rotor, the velocity in the area of the turbine shrinks. This fact agrees with the one-dimensional theory, where the average axial velocity keep reducing from upwind velocity v_1 to downwind velocity v_3 passing through the turbine with velocity, v.

The flatness and the smoothness in the velocity distribution are indications for the increasing of the mixing area between the wake and the surrounding, which indeed increases as we move downwind where the low pressure wake entrains more energy from surrounding.

The upwind velocity distributions of fine and coarse grids have the same trend the free flow turbulence, Figures 9 and 10. Hence, it is possible to define the reference upwind velocity for the all cases (no grid, fine grid and coarse grid).

Figures 11 and 12 show the velocity distribution behind the turbine with fine and coarse grids, respectively. It is apparent from the two figures and the previous Figure 8 that the downwind distribution of velocity is becoming flatter and smoother as the turbulence increases. In the wake of the rotor there is no significant difference, but the mixing border of the surrounding stream tube is becoming wider. At a very near distance of x/D = 0.2, the mixing is already starting at y/D = 0.54 and ends first at y/D = 0.8. Even at far distances, the mixing area continues to stay wider. The comparison of fig. 12 with Figures 8 and 11 shows this very clearly.

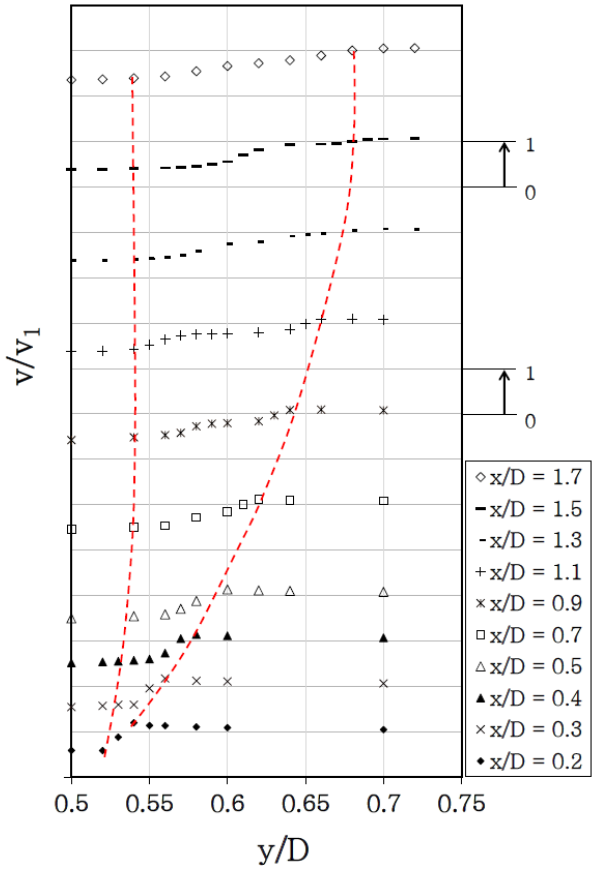


Figure 8. Downwind velocity distribution without grid, $v_1 = 12m/s$

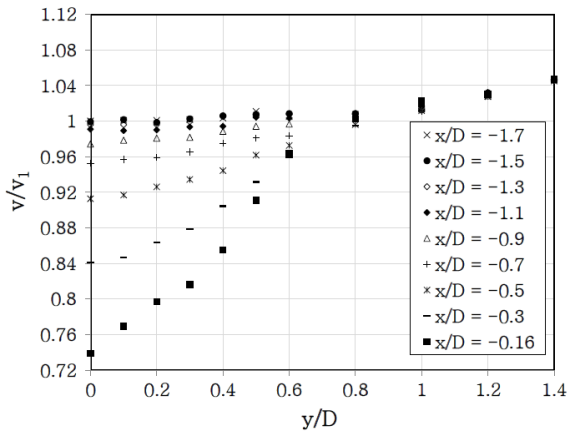


Figure 9. Upwind velocity distribution with fine grid at $v_1 = 12\ m/s$

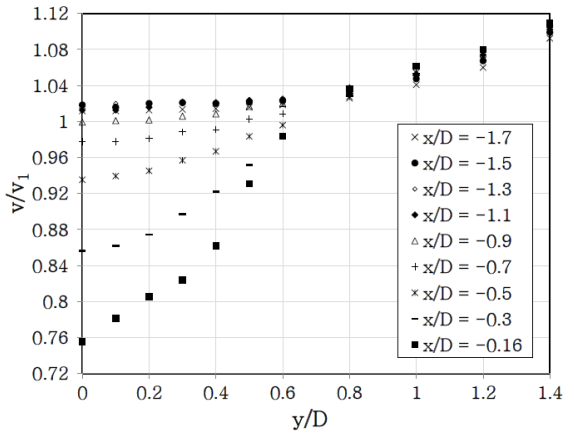


Figure 10. Upwind velocity distribution with coarse grid at $v_1 = 12\ m/s$

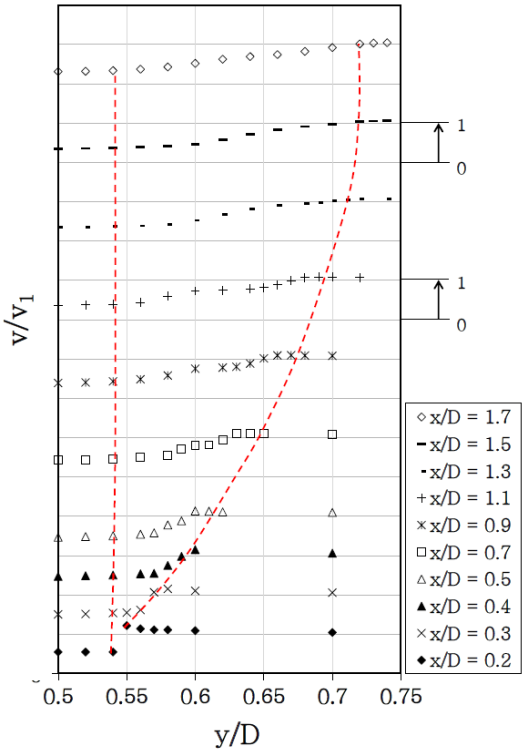


Figure 11. Downwind velocity distribution with fine grid, $v_1 = 12m/s$

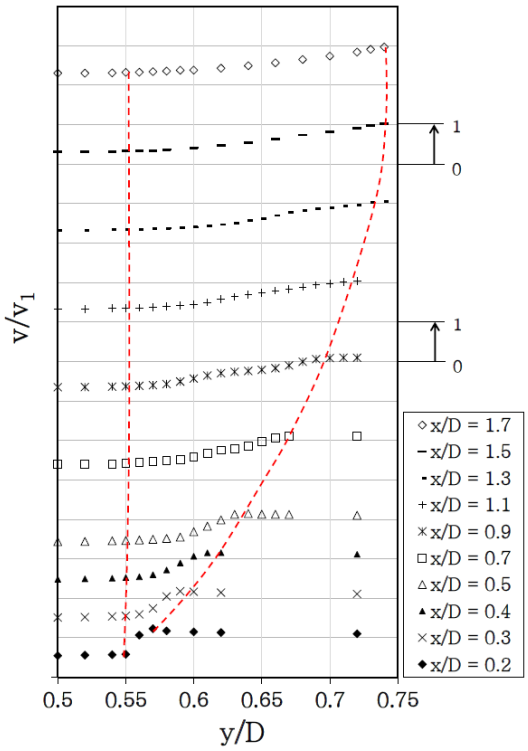


Figure 12. Downwind velocity distribution with coarse grid, $v_1 = 12m/s$

3.4. The Effect of Winglets

Previous investigations have shown an effect of turbulence on the power coefficient. The wake border reveal an increase in mixing with the increment of turbulent level. Analysis have shown an expansion of the wake stream tube downwind the turbine. There is an indication of a higher rotational speed caused by the turbulence. In order to isolate the major influence of tip vortex from other factors that possible contributes in the performance increment, it is suggested to add a winglet to the tip. Winglets suppose to reduce the tip losses by preventing the flow across and result in higher power extraction. Thus, different designs are tested until reaching a noticeable power increment.

The influence of winglets is restricted on the downwind area, thus, upwind measurements are not executed. Preliminary measurements show that the effect of winglet is not the same for all turbulence levels since the vortices are in different levels.

Results for higher turbulent levels (fine and coarse grids) showed no influence in C_p when adding winglet, thus, they are not presented here. This is because the tip vortices have already damped by the turbulence. Therefore, investigation of winglet is limited to the case of low turbulent level (no grid) to compare it later with higher turbulent levels.

Figure 13 shows the increment of C_p when using of winglet compared to the measurement without winglets at free flow turbulence (no grid). The gain is noticeable very clearly, but still the effect is less than the influence of adding turbulence when using of both fine and coarse grids as shown in the same figure. The comparison of the wakes in Figures 8, 11, 12 and 14 shows that the wake of the turbine with winglet is wider than the no winglet case and narrower wake than the turbulent cases. This comparison supports the C_p trend, because the wider the wake, the more the power extraction.

In comparison to Figure 8, there is a shift of the velocity mixing area to higher y/D at the inner, as well as the outer border. These results suggest that turbulence not only helps in suppressing the tip vortex,

but there are additional effects causing the rise in C_p. These might be boundary layer interaction with turbulence that led to delaying or damping the stall.

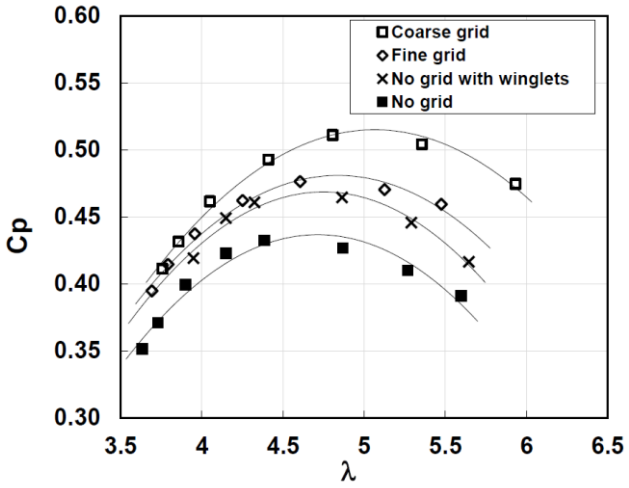


Figure 13. The effect of winglet on C_p at free flow turbulence (without grid). All cases at wind turbine position of *x=120 cm*

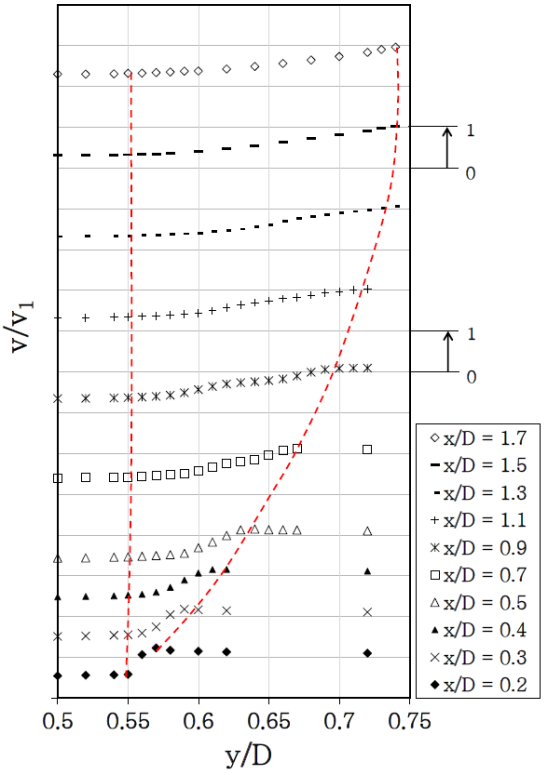


Figure 14. Downwind velocity distribution without grid and with winglet

3.5. Spectrum analysis

The same measured points of turbulent intensities in the previous section are used to measure the energy spectrum. Starting with the near wake distance of $x/D = 0.3$, Figure 15 shows the case when the

turbine is mounted at a test section position of 100 cm from the inlet of the test section, where the incoming turbulence intensities are known for different turbulent levels. It is possible to distinguish between energy developments as a function of eddies frequencies f at a different oncoming TI.

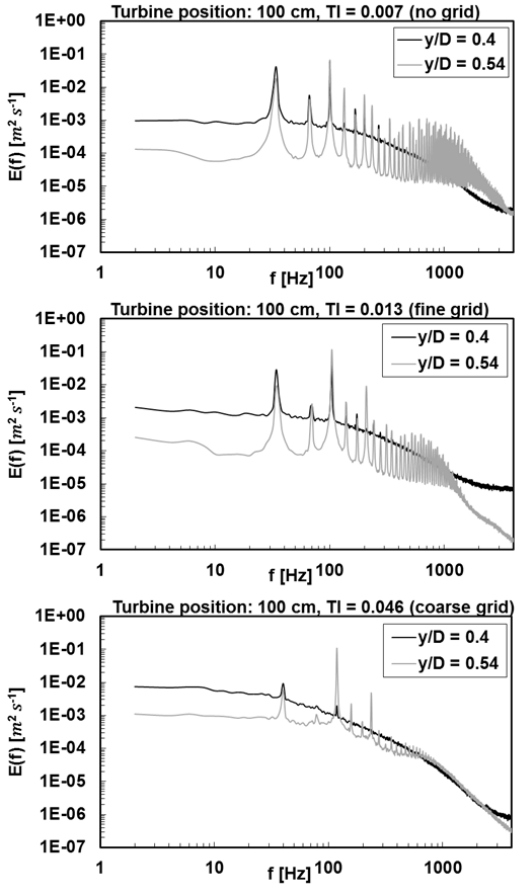


Figure 15. Spectra E(f) with eddies frequencies f at different radial distance y/D in the turbine wake with no-grid, fine and coarse grid incoming wind, hot-wire downwind position $x/D = 0.3$

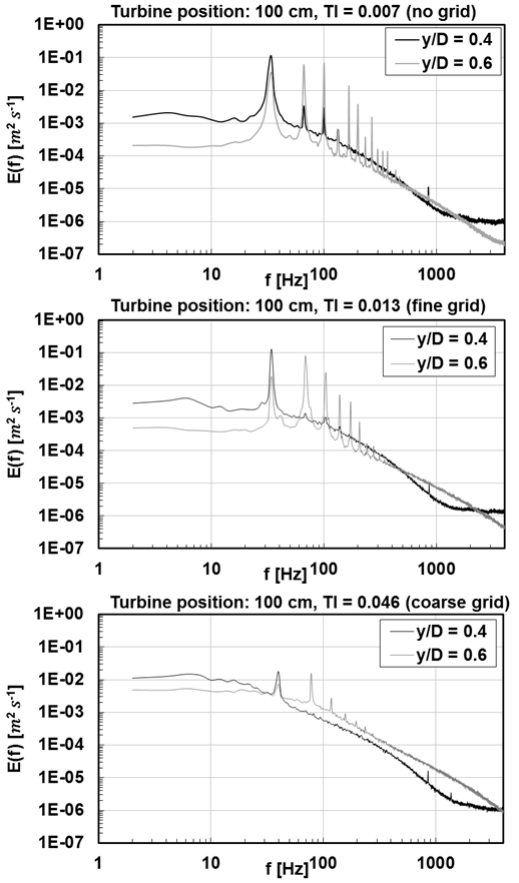


Figure 16. Spectra E(f) with eddies frequencies f at different radial distance y/D in the turbine wake with no-grid, fine and coarse grid incoming wind at hot-wire downwind position $x/D = 1.1$

In general, the energy of the most containing frequencies ($f \leq 100Hz$) increases. In analogy to the analysis of the downwind TI in the previous section, this increment is associated with the penetration of the incoming turbulence through the rotor plane. Figure 15 also shows three distinguished jumps of the energy at defined frequency (f $\approx$ 34, 66 and $100Hz$). These peaks correspond to the three rotor blades and represent the additional increment of TI (and thereby turbulent energy) of the rotation of the turbine.

The amplitude decays with increasing distance from the tip at y/D in both directions. Here, the mixing is most distinctive. With additional incoming grid-generated turbulences, the turbine rotates faster. This fact becomes clear in the figure by the shift of the peaks to higher frequencies.

Especially at the maximum fluctuation position for the low turbulent case, there is a high intensive mixing over a wide interval of frequencies. The effect fades with higher incoming turbulence, for the high turbulent case it is nearly completely disappeared. The fading is still noticeable when increasing measuring distance from the turbine Figure 16. Here, the three typical peaks still exist, but tip vortices are vanished through dissipation processes.

4. Conclusion

The present study aims at experimental investigating the Horizontal Axis Wind Turbines (HAWT) operating under the turbulence conditions. Hence, figuring out the impact of turbulence levels on the performance and wake of the HAWT. This is done by exposing an optimized HAWT model to turbulence with various energy content, which is generated by using two static squared grids.

For a systematic investigation of the turbulence influence on the wind turbine performance, a laboratory-scale HAWT that efficiently perform in a wind tunnel has been designed. It's efficiency is in the range of the real-scale HAWTs. Thus, the obtained measurements are reliable and possible to be reflected for various scales of HAWTs.

The higher the turbulence level the higher the power coefficient and hence the higher rotational speed for the same incoming wind velocity. Turbulence influences the performance throughout different means. Higher turbulence helps in damping the tip vortices. Thus, reduces the tip losses. In addition, adding winglets to the blade tip will reduce the tip vortex. The study has shown by adding winglets it is not possible to suppress all tip vortex.

Furthermore, high turbulence content in the incoming wind serves in increasing the wake-surrounding interaction, and hence more energy entrainment to the wake regime. More turbulent flow has been shown to penetrate through the turbine rotor plane, which brings different scales and hence more mixing in the near-wake regime. That in turns cause a faster of wake recovery.

5. Reference

[1] M. N. Nielsen S. C. Pryor P.-E. Rethore R. J. Barthelmie, S. T. Frandsen and H. E. Jrgensen, Modelling and measurements of power losses and turbulence intensity in wind turbine wakes at middelgrunden offshore wind farm. *WIND ENERGY*, 2007.

[2] Kurt S. Hansen, Rebecca J. Barthelmie, Leo E. Jensen, and Anders Sommer, The impact of turbulence intensity and atmospheric stability on power deficits due to wind turbine wakes at horns rev wind farm. *Wind Energy*, **15**(1):183-196, 2012.

[3] Matthias Türk and Stefan Emeisb. The dependence of offshore turbulence intensity on wind speed. *Journal of Wind Engineering and Industrial Aerodynamics*, 2010.

[4] K. E. Swalwell, J. Sheridan and W. H. Melbourne, The effect of turbulence intensity on stall of the NACA 0021 Aerofoil, 2001.

[5] F.A. BACCHI J. COLMAN J.S. DELNERO, J. MARAON DI LEO and U. BOLDES. Experimental determination of the influence of turbulent scale on the lift and drag coefficients of low Reynolds number airfoils. *Latin American Applied Research*, 2005.

[6] S. Ravi S. Watkins and B. Loxton. The effect of turbulence on the aerodynamics of low Reynolds number wings. *Engineering Letters*, 2010.

[7] J. MURATA T. TOKI Y. KAMADA, T. MAEDA and A. TOBUCHI. Effects of turbulence intensity on dynamic characteristics of wind turbine airfoil. *Journal of Science and Technology*, 2011.

[8] K Mikkelsen, Effects of turbulence intensity on power output of wind turbine operating in wake, 2010.

[9] Leonardo P. Chamorro and Fernando Portè-Agel. A wind-tunnel investigation of wind-turbine wakes: Boundary-layer turbulence effects. *Boundary-Layer Meteorol*, 2009.

[10] Thogersen M Frandsen S. Integrated fatigue loading for wind turbines in wind farms by combining ambient turbulence and wakes. *Journal of Wind Energy*, 1999.

[11] Verification of a new model to calculate turbulence intensity inside a wind farm, 2006.

[12] M. R. Luhur, M. Wchter, and J. Peinke. Stochastic modeling of lift and drag dynamics under turbulent conditions. *European Wind Energy Conference and Exhibition 2012, EWEC 2012*, volume **1**, pages 432-438, 2012.

[13] B. Stoevesandt and J. Peinke. Changes in angle of attack on blades in the turbulent wind field. volume **6**, pages 4329-4332, 2009.

[14] F. Böttcher D. Heinemann B. Lange J. Peinke, S. Barth. Turbulence, a challenging problem for wind energy. *Journal of Physica A*, 2004.
[15] A. Al-Abadi, F. Beyer, A. Delgado, Ö. Ertunc. Torque-matched aerodynamic shape optimization of HAWT rotor. *Journal of Physics: Conference Series*, **555**(2014) 012003.
[16] Ali Al-Abadi, Özgür Ertunç, Philipp Epple, Wolfram Koerbel, Antonio Delgado, DEVELOPMENT OF AN EXPERIMENTAL SETUP FOR DOUBLE ROTOR HAWT INVESTIGATION, Bella Center, *Proceedings of ASME Turbo Expo*. Copenhagen, Denmark, June, 2012.
[17] Özgür Ertunc. Experimental and Numerical Investigations of Axisymmetric Turbulence. PhD thesis, Friedrich-Alexander University, Germany, Erlangen, 2006.
[18] Durst, Franz, Grundlagen der Strömungsmechanik. Springer-Verlag, Berlin, Heidelberg, 2006.
[19] Stephen B. Pope, Turbulent Flows. Cambridge University Press, 2000.
[20] Wind turbines – Part 2: Design requirements for small wind turbines (IEC 61400-2:2006), European Committee for Electrotechnical Standardization
[21] IEC 61400-1, Wind turbines – Part 1: Design requirements, Ed.3, 2005.

Acknowledgments
This study was partially supported by BB21 Project, Busan Metro Politian City, South Korea.